



Bark and biochar in horizontal flow filters effectively remove microplastics from stormwater

Rullander, Gabriella; Lorenz, Claudia; Strömvall, Ann Margret; Vollertsen, Jes; Dalahmeh, Sahar S.

Published in:
Environmental Pollution

DOI (link to publication from Publisher):
[10.1016/j.envpol.2024.124335](https://doi.org/10.1016/j.envpol.2024.124335)

Creative Commons License
CC BY 4.0

Publication date:
2024

Document Version
Publisher's PDF, also known as Version of record

[Link to publication from Aalborg University](#)

Citation for published version (APA):
Rullander, G., Lorenz, C., Strömvall, A. M., Vollertsen, J., & Dalahmeh, S. S. (2024). Bark and biochar in horizontal flow filters effectively remove microplastics from stormwater. *Environmental Pollution*, 356, Article 124335. <https://doi.org/10.1016/j.envpol.2024.124335>

General rights

Copyright and moral rights for the publications made accessible in the public portal are retained by the authors and/or other copyright owners and it is a condition of accessing publications that users recognise and abide by the legal requirements associated with these rights.

- Users may download and print one copy of any publication from the public portal for the purpose of private study or research.
- You may not further distribute the material or use it for any profit-making activity or commercial gain
- You may freely distribute the URL identifying the publication in the public portal -

Take down policy

If you believe that this document breaches copyright please contact us at vbn@aub.aau.dk providing details, and we will remove access to the work immediately and investigate your claim.



Bark and biochar in horizontal flow filters effectively remove microplastics from stormwater[☆]

Gabriella Rullander^{a,*}, Claudia Lorenz^b, Ann-Margret Strömvall^c, Jes Vollertsen^d, Sahar S. Dalahmeh^a

^a Department of Earth Sciences, Uppsala University, Villavägen 16, SE-752 36, Sweden

^b Environmental Dynamics, Department of Science and Environment, Roskilde University, Universitetsvej 1, 11.2 DK-4000, Roskilde, Denmark

^c Water Environment Technology, Department of Architecture and Civil Engineering, Chalmers University of Technology, SE-412 96, Gothenburg, Sweden

^d Aalborg University, Department of The Built Environment, Thomas Manns Vej 23, 9220, Aalborg Øst, Denmark

ARTICLE INFO

Keywords:

Filter solutions
MP
Particle transport
Porous material
μ-FTIR
Stormwater management

ABSTRACT

Organic materials such as bark and biochar can be effective filter materials to treat stormwater. However, the efficiency of such filters in retaining microplastics (MPs) – an emerging stormwater pollutant – has not been sufficiently studied. This study investigated the removal and transport of a mixture of MPs commonly associated with stormwater. Different MP types (polyamide, polyethylene, polypropylene, and polystyrene) were mixed into the initial 2 cm material of horizontal bark and biochar filters of 25, 50, and 100 cm lengths. The MP types consisted of spherical and fragmented shapes in size ranges of 25–900 μm. The filters were subjected to a water flow of 5 mL/min for one week, and the total effluents were analyzed for MPs by μFTIR imaging. To gain a deeper insight, one 100 cm bark filter replica was split into 10 cm segments, and MPs in each segment were extracted and counted. The results showed that MPs were retained effectively, >97%, in all biochar and bark filters. However, MPs were detected in all effluents regardless of filter length. Effluent concentrations of 5–750 MP/L and 35–355 MP/L were measured in bark and biochar effluents, respectively, with >91% of the MP counts consisting of small-sized (25 μm) polyamide spherical particles. Combining all data, a decrease in average MP concentration was noticed with longer filters, likely attributed to channeling in a 25 and 50-cm filter. The analyses of MPs in the bark media revealed that most MPs were retained in the 0–10 cm segment but that some MPs were transported further, with 19% of polyamide retained in the 80–90 cm segment. Overall, this study shows promising results for bark and biochar filters to retain MPs, while highlighting the importance of systematic packing of filters to reduce MP emissions to the environment from polluted stormwater.

1. Introduction

Stormwater management can be challenging in urban environments, as the presence of impermeable surfaces (e.g., roads, roofs, and parking lots) coupled with dense populations, can intensify both the runoff from rain events and the anthropogenic pollution following human activities. This runoff, known as stormwater, can carry various pollution e.g., bacteria, metals, nutrients, organic contaminants, and emerging contaminants like microplastics (MPs), which can pose hazards to the aquatic environment if left untreated (Biswal et al., 2022). MPs, plastic items <5 mm, have gained recent attention as stormwater pollutants due to their persistent nature, tendency to serve as carriers for other toxins,

pathogens, and pollutants, and their potential to leach chemical additives over time (Coyle et al., 2020). To address issues of urban stormwater pollution and mitigate the risks of flooding (Bibi & Kara, 2023) and contamination of aquatic systems, many countries have implemented stormwater management strategies.

In the effort to enhance the removal of stormwater pollutants, filtration-based stormwater management techniques are growing in popularity (Chandrasena et al., 2017; Kuoppamäki et al., 2021). These units often consist of depressions that store stormwater and improve its quality by allowing the water to percolate through a filtration media, traditionally a mix of sand and soil, to capture and treat the stormwater (Payne et al., 2015). It is recognized that the choice of filter material is

[☆] This paper has been recommended for acceptance by Dr Michael Bank.

* Corresponding author.

E-mail address: gabriella.rullander@geo.uu.se (G. Rullander).

the key parameter that determines pollutant removal (Hunt et al., 2012). Traditional filtration units have shown sufficient removal of suspended solids, nutrients, and some metals (Davis et al., 2009; EPA, 1999; Goor et al., 2021). However, to improve performance and optimize the removal of a wider range of pollutants associated with urban stormwater, researchers are increasingly investigating amended filters and the incorporation of materials with enhanced sorption qualities (Björklund & Li, 2015; Li et al., 2010; Markiewicz et al., 2020). Yet, there are few studies examining the efficiency and processes of MP retention by such filter units.

Biochar have gained recognition as a sorption and filter media due to their unique material properties, such as water-holding capacity, porosity, hydrophobicity, and large surface area (Spokas, 2010; Weber & Quicker, 2018). Biochar can exhibit aromatic structures, functional groups, and surface characteristics which can enable the sorption of organic pollutants through mechanisms like hydrophobic attraction and van der Waals electrostatic interaction (Bansal & Goyal, 2005; Mohanty et al., 2018), providing effective removal of polycyclic aromatic hydrocarbons (PAHs), among other trace organic pollutants (Ashoori et al., 2019; Reddy et al., 2014; Ulrich et al., 2015). The high pore volume and specific surface area of biochar have also contributed to the effective sorption of per- and polyfluoroalkyl substances (PFAS; Krahn et al., 2023), while demonstrating significant sorption potential for dissolved metals (Li et al., 2017; Milovanovic et al., 2023).

Bark, characterized by its porosity and rich content of natural organic compounds such as cellulose, polysaccharides, lignin, and tannin has also been utilized in filter studies (Björklund & Li, 2015; Brás et al., 2004; Li et al., 2010). The lignin present in bark can encompass both aromatic groups and hydrophobic surface groups, thereby potentially facilitating the removal of both hydrophilic and hydrophobic pollutants (Valentín et al., 2010). PAHs, which are prone to hydrophobic partitioning in sorption material, have shown to be efficiently removed in the upper layer of vertical bark filters (Markiewicz et al., 2020). The utilization of bark and biochar as stormwater filter media is also considered environmentally beneficial, as these low-cost materials contribute to carbon sequestration. However, knowledge gaps remain to be answered regarding the materials' potential to remove MPs from stormwater.

Only a few studies have investigated MP retention using vertical biochar filters. Wang et al. (2020) found that amending sand filters with biochar produced from corn straw and hardwood at temperatures of 500 °C resulted in the removal of more than 90% of polyethylene (PE, 10 µm) through physical entrapment and entangling within the filter media. In contrast, Siipola et al. (2020), who performed a study with steam-activated biochar produced from pine and spruce bark during slow pyrolysis at 475 °C, showed that this filter was unable to retain PE (10 µm). Instead, the filter material provided the removal, >90%, of fibers and PE pieces measuring 2–3 mm through physical attachment. While physical attachment plays a key role in MP retention, smaller MPs of polystyrene (PS, 1 µm), have also been efficiently removed, 98.8–99.6%, in magnetic modified biochar. This removal was attributed to electrostatic interaction and chemical bonding (Wang et al., 2021). Hence, the removal efficiencies of MPs appear to vary depending on the MP type and the biochar feedstock and its applied production technique (i.e. temperature, duration, and/or alterations via biochar activation). In terms of utilizing bark as a filter media, no scientific articles related to MP removal have been published, to the authors' knowledge. However, it can be argued that the removal of PAHs found in bark filters (Markiewicz et al., 2020) is of interest for MP studies, as the organic compound has been used as an additive for tire production (Arole et al., 2023) and found leaching from discarded cigarette butts in the environment (Dobaradaran et al., 2020). Similarly, a recent study by Wang et al. (2023) found that wood residues (sawdust) coated with natural phenols effectively, >99.9%, removed a diverse mixture of nanoplastics (NPs) and small-sized MPs (100 nm–22 µm) in flow-through vertical filters, attributed to surface adsorption through multi-molecular

interactions. Thus, bark material, which can contain phenolic acids (e.g., tannins), is a promising candidate for MP removal with the potential to remove small-sized MPs through both physical interception and surface adsorption.

This paper aims to investigate whether commercially available pine bark and biochar constitute porous materials that can be utilized in stormwater filters to enhance the removal of MPs from the water. Specifically, this study first investigates the overall retention of a mixture of MPs in lab-scale horizontal flow filters of pine bark and biochar and evaluates the impact of MP characteristics on the retention. Secondly, it assesses the transport of MPs in response to a continuous horizontal infiltration by introducing different filter lengths (25, 50, and 100 cm). Finally, the spatial retention of MPs in response to the horizontal water movement is evaluated by dissecting and quantifying MPs in 10 cm segments of a 100 cm bark filter.

2. Method and materials

2.1. The organic filter material characterization

Commercially sold biochar (Vindelkol AB, Sweden) and pine (*Pinus Sylvestris*) bark (Plantagen, Sweden) were used in the experiment. The biochar was produced through the pyrolysis of a feedstock dominated mostly by pine, followed by birch, alder, and aspen hardwood at 500 °C for approximately 8–14 h (Vindelkol AB, Sweden).

The bark and biochar were oven-dried and then sieved manually, discarding particles smaller than 0.5 mm and larger than 4.5 mm. The particle size distributions of bark and biochar material were determined by transferring a portion of the materials to a stack of metal sieves ranging from 0.063 to 16 mm, in a sieve shaker (E.V.J. 1. Endecotts, England) for 30 min. The materials contained in each fraction were weighed and the cumulative percentage finer was presented as particle size distribution curves. The effective size (D10) showed that 10% of the bark particles were finer than 0.7 mm and, for biochar, 10% of the particles were finer than 1.3 mm (Fig. 1). The D30 and D60 were determined as 1.6 and 2.6 mm for bark and 2.1 and 2.9 mm for biochar, respectively. The coefficient of uniformity (Cu), was higher than 1 for both materials, indicating a wider range of particle sizes in the materials, where biochar (Cu = 2.19) had a slightly narrower range than bark (Cu = 3.7), see also Supplementary Information S1. The coefficient of curvature (Cc), was close to 1 for both materials, indicating a close to symmetrical distribution. Both materials were classified as poorly graded, with a range of particle sizes, with relatively symmetrical

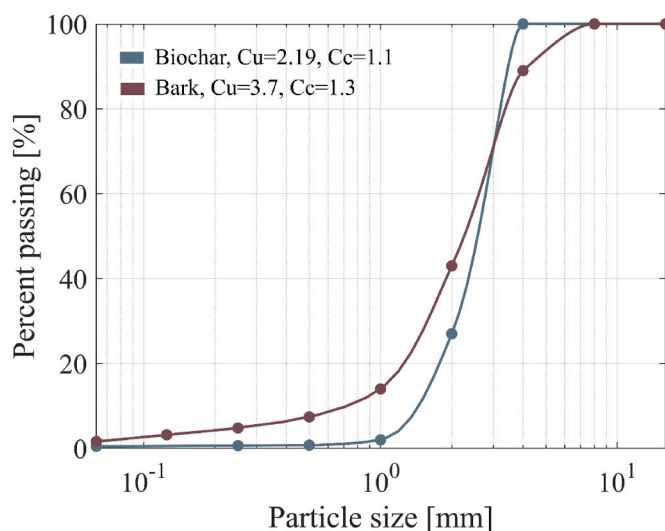


Fig. 1. Particle size distribution of bark and biochar with passing cumulative weight percentage of the sieved material which passed a given sieve size.

particle size distributions.

The elemental composition and surface shape morphology of samples of the bark and biochar were determined using field emission Scanning Electron Microscopy (SEM, Zeiss Supra 35-VP microscope, Carl Zeiss SMT, Oberkochen, Germany; see Fig. 2) coupled to energy dispersive spectroscopy. An example of SEM images of the bark and biochar used in this study is provided in Fig. 2 and a summary of the percentual carbon and oxygen composition is presented in Table 1. It is seen in Fig. 2 that the biochar is a porous material with a high specific surface, also confirmed by the measurement of the Brunauer-Emmett-Teller (BET) method, on which the average pore diameter of the materials was determined (Table 1).

The pore volume of each packed filter was estimated by registering the volume of water required to saturate the porous media. For details on estimations of the particle and bulk densities, porosity, and pore volume of the material and filters (see Supplementary Information S2).

2.2. Experimental set-up

Polyvinyl chloride (PVC) tubes (diameters of 4.6 cm) were packed separately with bark and biochar. For each material, three filter lengths (25, 50, and 100 cm) were used and three replicas were prepared for each length (i.e., in total 9 filters per material). See Rullander et al. (2023) for a detailed description and schematics of the experimental setup. The tubes were gently packed with bark or biochar, in a vertical position, then placed horizontally and washed with tap water for 1 week at a constant flow of 5 mL/min using a peristaltic pump (Masterflex L/S Labinette, Sweden).

Of the three replicas, one was used to conduct a tracer test and to evaluate the potential MP contamination from media (biochar and bark) or the supplied water (tap water). All filters were run with regular tap water to imitate a natural ion balance for the filter beds while simulating runoff water without the interference of metals or other organic contaminants otherwise associated with naturally obtained stormwater.

2.3. Tracer test

The hydraulic residence time of the filters was determined for control filters of bark and biochar through tracer tests, where a sodium chloride (NaCl, 5 and 30 g/L) solution was added as a pulse (300 mL, 5 mL/min), measuring 20–100 times higher values than the background conductivity. During the test, the effluents were accumulated and the electrical conductivity of the accumulative volume was measured every 5 min (Cond 3310, WTW) with a conductivity probe (Tetracond 325, WTW). The salt mass corresponding to the measured conductivity was determined and the mean residence time was assigned to the time when 50% breakthrough of the total injected salt mass was reached (see also

Supplementary Information S3).

2.4. Transport of microplastics under horizontal flow conditions

Of the three prepared replicate filters, two were used to investigate the transport of spherical polyamide (PA; 10–50 μm , $D_{50} = 25 \mu\text{m}$; Goodfellow, England), irregularly shaped polypropylene (PP; 20–150 μm , $D_{50} = 63 \mu\text{m}$; Goodfellow, England), spherical polyethylene (PE; 105–145 μm , $D_{50} = 125 \mu\text{m}$; Sigma-Aldrich, Germany), and polystyrene beads (PS; $D_{50} = 900 \mu\text{m}$; Goodfellow, England) with comparable densities (PA: 1.020 g/cm³, PP: 0.90 g/cm³, PE: 0.94 g/cm³, PS: 1.05 g/cm³) in a continuous horizontal flow mode. The spherical MPs (PA, PE, and PS) were purchased ready-made, and fragments were obtained by shredding larger PP beads in a stainless-steel food processor, together with liquid nitrogen (for further information see Rullander et al., 2023).

Using a metal spoon, the initial 2 cm of the inlet zone of the washed filter media was removed from the packed tubes, transferred to glass beakers, and then mixed with 0.07 g each of PA, PE, and PP and 0.5 g of PS MPs. Then, the homogenized mixture was replaced in the filter inlets. The utilized glass beakers were carefully rinsed with ethanol three times, and this liquid was also transferred to the filters. A standard of the MP-mixture was analyzed by μFTIR imaging and the MP counts and weights of each added polymer were estimated based on these measurements.

Once the MP-mixtures were added to the inlet zones, the horizontal filters received a constant flow (5 mL/min) of tap water, leading to a surface loading rate of 180 mm/h, for one week. The flow rate was within the rates found appropriate for suspended solid removal in conventional stormwater filtration units (Davis et al., 2009; Hunt et al., 2012). The effluent water was accumulated during the one-week experiment, and the MPs in the accumulative volume (50.4 L) were then extracted and analyzed using μFTIR imaging.

The horizontal distribution of MPs, in the longitudinal direction of flow, was studied by utilizing distinct filter lengths 25, 50, and 100 cm, and analyzing the cumulated MP effluents. Analyzing the MP effluent after a certain thickness of filter material, instead of analyzing MPs retained in filters at different locations, was favored because of difficulties with extracting MPs from biochar and bark material. This difficulty relates to the intense capture of MPs within the pores, and the light weight of the materials which complicates density separation methods. Additionally, the black carbon found in biochar makes it unsuitable for μFTIR imaging (Wagner et al., 2018). Nevertheless, upon completion of the experiments, the bark material from the second 100 cm replica was dissected into 10 cm segments using a stainless-steel saw, and the MPs were extracted and analyzed from each section of the total sample. This was done to provide an insight into the spatial distribution of MPs in the media (i.e. transport of MPs along the filter length in response to the surface loading).

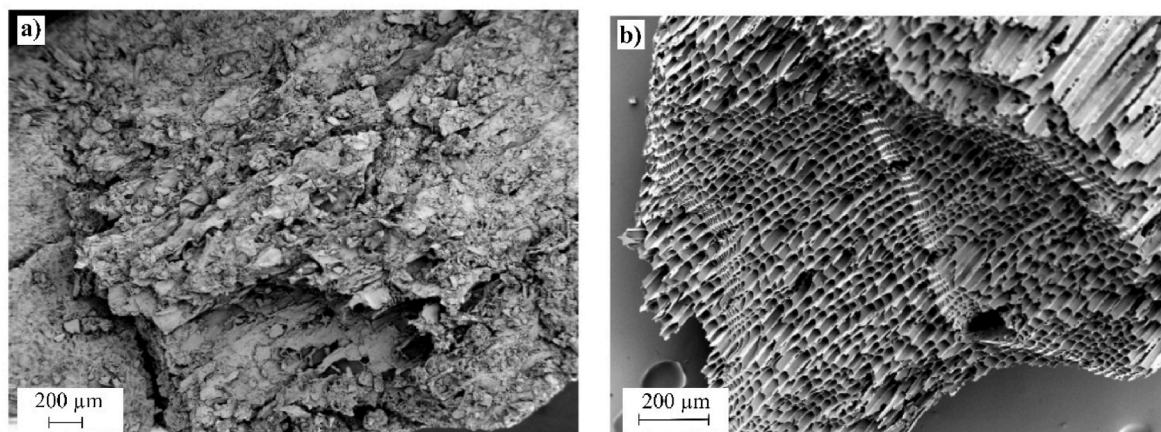


Fig. 2. The surface morphology of a) bark and b) biochar was determined using a Scanning Electron Microscope.

Table 1

The surface characteristics of biochar and bark, and the average pH measured in effluent water at the start and end of the experiment (one week).

Media Characteristics					Effluent pH	
Material	Porosity, f (%)	Specific surface area (m^2/g)	Average pore diameter, (nm)	Elemental composition of carbon, C, and oxygen, O (%)	pH initial	pH final
Biochar	87 ± 0.010	158 ± 1.77	3.60	C 86.2	7.7	8.1
				O 12.9		
Bark	75 ± 0.031	0.75 ± 0.0050	17.2	C 57.4	4.7	7.4
				O 33.3		

2.5. Microplastic extraction

The MPs were extracted from the accumulated effluents of the biochar and bark filters via vacuum filtration on 10 μm stainless steel filters. The filters were transferred to glass beakers, submerged in pure ethanol, and covered with aluminum foil, then sonicated for 15 min to detach the MP particles. After detaching the MPs from filters, the MP-ethanol suspensions were transferred to 20 mL glass vials, and the ethanol was evaporated, under a gentle nitrogen gas flow, until dry. Then, 2 mL ethanol was added to glass vials. The final 2-mL MP-ethanol suspensions of all samples were stored at fridge temperatures.

To separate the MPs from the 10 cm bark segments, wet-sieving, removal of organic matter by Fenton's reagent oxidation, and density separation were applied following methods derived from Liu et al. (2019), Simon et al. (2018), and Masura et al. (2015). In short, each 10 cm segment of the bark filter was stored in glass beakers and then wet-sieved on metal sieves of 1500 μm and 300 μm mesh size. All bark retained on the 1500 μm sieve was discarded. Whilst, the bark retained on the 300 μm was saved and the 900 μm PS beads were manually recovered, using metal forceps.

The matrix (water, bark, and MPs) which passed the 300 μm sieve was collected for each segment and then vacuum-filtered through 10 μm stainless steel filters. The metal filters were transferred to glass beakers, covered with de-ionized water, and sonicated for 15 min. The sonicated residues except the stainless-steel filters were then transferred into larger beakers to which 345 mL 30% H_2O_2 and 65 mL 0.1 M NaOH and gradually 62 mL 0.1 M FeSO_4 were added while the beakers were submerged in an ice bath. The exothermic Fenton-reaction was observed for 4 h, maintaining the sample temperatures around 30 $^\circ\text{C}$. The reactions were left to continue for 24 h, after which an additional 62 mL H_2O_2 was added to each sample, and the samples were left for another 24 h. Then, the samples were filtered on 10 μm stainless steel filters. The metal filters together with retained material were transferred to large glass beakers, adding two-thirds of the beaker volume with dense ZnCl_2 salt solution, 1.4 g/cm^3 , and mixing the samples vigorously with a metal spoon for 5 min. The solutions were left to settle for 24 h, after which the supernatants were filtered on 10 μm stainless steel filters, using a vacuum. The density separation was repeated three times in total. The final filters containing the extracted MPs were transferred to glass beakers, immersed in pure ethanol, and sonicated for 15 min. Finally, the MP suspension volume was evaporated and fixed at 2 mL. As a recovery experiment, saturated bark of the same volume as a bark segment (166 cm^3) was spiked with 100 PS beads, and extracted according to the extraction method used for the bark segments as described above (see also Supplementary Information S4 for a schematic overview of extraction method).

2.6. Microplastic identification and quantification

100 μL sub-samples of the 2 mL MP-ethanol suspensions were transferred to zinc selenide optical windows (Crystran, UK), which were placed in a micro compression cell (Pike Technologies, USA), thus restricting the active surface to a diameter of 10 mm. Two sub-samples of each suspension were analyzed, resulting in an analysis of 10% of the total sample volume. Before analysis, the windows were dried at 40 $^\circ\text{C}$ on a heat plate and scanned (μFTIR imaging) at a pixel resolution of 5.5

μm using a Cary 620 FTIR microscope equipped with a 64x64 Focal Plane Array (FPA) detector coupled with a Cary 660 IR spectrometer (Agilent Technologies, USA), which had a 15x Cassegrain objective. The entire active surface of each window was scanned in transmission mode at a spectral range of 3750–950 cm^{-1} , at 8 cm^{-1} resolution, and with 16-coadded scans (Olesen et al., 2019; Simon et al., 2018). The resulting IR maps were analyzed in siMPle v.1.3.1 β (Systematic Identification of MicroPlastics in the Environment) freeware (Primpke et al., 2020). The library applied as a reference for the IR maps contained spectra of various standard plastics (Vianello et al., 2019), and organic materials, with added spectra of the MPs utilized in the experiment. The identified MPs were quantified with the siMPle software. Additionally, siMPle provided estimations of the MP mass, based on an assumption of particle thickness, elliptical shape, and the theoretical density of the polymer type (siMPle, 2022). Thus, this study provided information on the quantified MP counts and their estimated mass. Additionally, a standard of the MP-mixture was prepared and diluted with 20 mL ethanol, and a subsample of 20 μL was analyzed with μFTIR imaging, before being processed with the siMPle software. Thereby, providing particle counts and estimated weights of each polymer added in the initial filter inlets. This was done to increase the comparability between the effluent MP concentrations and the MPs mixed in the initial layer (0–2 cm) of the filter inlet. Expressing MP concentrations through both count and mass estimations enhances comparability with other studies, regardless of whether they report MP data in counts or mass. This standard MP-mixture included all MPs apart from PS beads, which could not be analyzed with μFTIR due to their size (900 μm). Throughout this study, PS beads are therefore referred to in terms of actual counts and weights.

2.7. Contamination control

As MP pollution is present in the air, and plastic materials are frequently common, great care was taken to exclude the external impact of MPs during experiments and analysis. Lab materials utilized during the extraction were made either from glass or metal, and sterilized before usage, and the in- and outlets of the filters, as well as the stainless-steel buckets collecting effluents, were covered with aluminum foil throughout the experiment. Given that the filter tubes were built in PVC material, this polymer was not included in the mixture of MPs distributed in the initial layer of filter inlets, and it was excluded from the analysis. Still, excluding all external influences of plastic was difficult, as biochar and bark materials were purchased and packaged in plastic bags for shipping. Therefore, it was important to include control filters with the materials and analyze potential background contamination of MPs from the porous media, as well as the tap water. For each control system, a total cumulative effluent of around 151 L was filtered and analyzed for MPs.

2.8. Data handling

The analyzed MP counts and masses quantified in sub-samples were extrapolated to represent full sample sizes. Due to the heterogeneity and individuality of MP background contamination in bark and biochar materials, pursuing blank corrections was deemed inappropriate. Instead, the background contamination from the control filters of bark and biochar are presented separately. All figures and data were

processed in MATLAB R2021a.

3. Results and discussion

3.1. Microplastics in the initial layer of filter inlets

This study controlled the placement and concentrations of MPs mixed within the initial layers of the filter media, chosen for their relevance in urban stormwater. The MPs were mixed into the 2 cm initial layer of the filter inlets, aligning with findings that MPs tend to concentrate in upper layers in treatment filters or terrestrial soil (Park et al., 2023; Zhang et al., 2022). Within this layer, MP counts ranged from 2.5×10^3 – 1.9×10^6 , corresponding to an estimated mass of 20–110 mg of PA, PE, and PP (<300 μm) and 0.5 g of PS beads (>300 μm), see Fig. 3. In total, 50.4 L of tap water was passed through the filters, corresponding to a count concentration of 50–37,700 MP/L or an estimated mass concentration of 400–2200 $\mu\text{g/L}$ each of PA, PE, and PP, along with 10 mg/L of PS beads.

Note that mass and particle counts for PA, PE, and PP were estimated using μFTIR imaging, while the largest PS beads (900 μm) were based on actual weights and manual counts (Fig. 3). The MP concentration in this experiment may be considered high compared to real stormwater. Yet similar MP loads have been used in previous studies on MP mobility in vertical soil columns (O'Connor et al., 2019), and comparable MP abundances have been measured in urban stormwater treatment facilities. For instance, a study in Sweden found MP masses ranging from 8.4 to 580 $\mu\text{g/L}$ in a stormwater chamber, when analyzing MPs >10 μm and including tirewear particles (Johansson et al., 2024).

Even higher concentrations of MPs have been found in stormwater

sediments, where MPs have settled over time (Liu et al., 2019; Olesen et al., 2019; Zhang et al., 2024). For example, MP counts ranging from 10^3 – 10^6 per kg of sediment were found in urban stormwater basins in France, while including particle-sizes of 50–500 μm (Iannuzzi et al., 2024). In general, high variability of MP concentration is a common denominator for stormwater samples, with reported MP counts ranging from 1 to 8500 MP/L (Järslskog et al., 2020; Ross et al., 2023; Sang et al., 2021; Sun et al., 2023). This variability can also be noted for MPs quantified in urban road dust, a source expected to transport a portion of the MPs in stormwater after rain events (O'Brien et al., 2021). For instance, Monira et al. (2022) quantified 520–1130 MPs per kg road dust from an urban catchment in Australia, with 17–33 MP/L MPs identified in stormwater.

The thermoplastics (PA, PE, PP, and PS) utilized in this study have commonly been identified in stormwater (Lange et al., 2021; Liu et al., 2019; Olesen et al., 2019), reflecting their statuses as some of the most commonly produced polymers. The pollution of such polymers can be seen in diverse sites of the world. For instance, PP, PE, PA, PS, PET, PU and PVC are among the most abundant MP types found in stormwater basins in France (Iannuzzi et al., 2024) and similarly, PE, PP, PA, PET and PS were identified in road dust samples from Queensland, Australia (Monira et al., 2022). Due to weathering in the environment, secondary MPs with fragmented shapes are often characterised in environmental samples (Amenábar et al., 2024), prompting the inclusion of PP fragments in the experiment. Moreover, it has been established that MP abundance in environmental samples tends to increase with decreasing particle size (Enders et al., 2015), with many studies including size ranges of 10–2000 μm (Liu et al., 2019; Monira et al., 2022; Zhang et al., 2024). In this study, four MP types in size ranges of 25–900 μm were

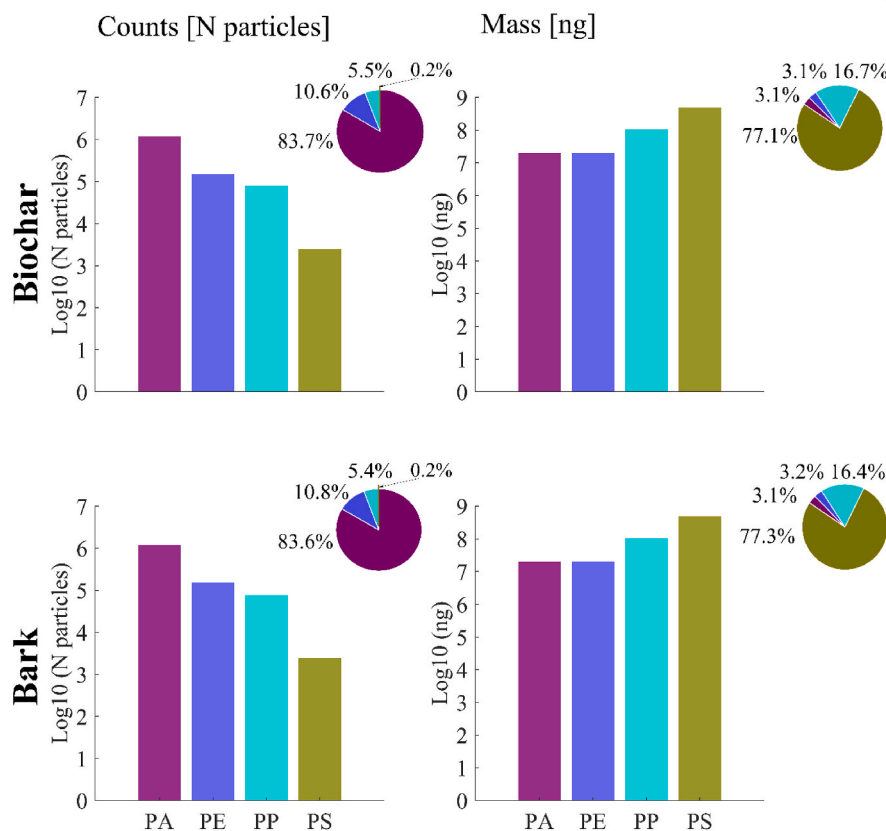


Fig. 3. The average counts and masses of MPs mixed in the initial layer (0–2 cm) of biochar and bark filters of all lengths (25, 50, and 100 cm). The average is calculated for 6 number of samples. The piecharts represent the polymer distribution of the average MP count and mass in the initial inlet zone of all filter lengths.

introduced with equal weights, thus providing a greater particle count for small-sized (25 μm) PA (Fig. 3).

3.2. Microplastics in bark and biochar filter effluents

For each control system of the filters, results indicate that bark and biochar filters released 10 and 7.6 MP/L, respectively. Of these identified MPs, 24–30% represented MPs not utilized in the experiment, such as polyethylene terephthalate (PET) fibers, PVC, and poly (methyl methacrylate) (PMMA) MPs (for further information see [Supplementary Information S5](#)). The background concentrations were higher than expected, but not surprising given that the bark and biochar materials were packed in plastic bags for shipping, and the storage conditions prior to purchase was unknown. This suggests that the materials could have been exposed to atmospheric deposition among other external sources of MP contamination. After one week of operating the filters at 180 mm/h, 50.4 L of effluent had passed through the filters and MPs had exited to all effluents with counts and masses ranging from 35 to 355 MP/L, equivalent to 870–4460 ng/L, for biochar filters and 5–750 MP/L, equivalent to 70–62900 ng/L, for bark filters (Fig. 4). Compared to the distribution of MPs in the initial layer (Figs. 3), 47–94% of the average weights and counts of MPs analyzed in all filter effluents comprised small-sized spherical PA particles (Fig. 4), with no large-sized PS beads passing through any filter. The results of this study share similarities to those of [Park et al. \(2023\)](#) where 2.7 g of fragmented PP (100–1000 μm) MPs were introduced into the initial layer of 22 cm vertical sand filters. A total of 37 L of effluent passed through the filters over two weeks, resulting in a count of 1.7 MP/L in the effluent, with most MPs retained in the upper layer (3.4 cm). In our study, PP fragment concentrations of 1.4–33 MP/L were observed in effluents from 25 cm horizontal biochar and bark filters.

Recent literature has suggested that the transport of MPs in vertical filters is neither governed by the infiltration volume nor the MP concentration placed in the initial filter layer ([O'Connor et al., 2019](#)); instead, evidence points to a flow-intensity-dependent transport of MPs ([Zhang et al., 2022](#)). The utilization of higher infiltration rates in our study compared to [Park et al. \(2023\)](#), still yielded a similar range of PP fragments in the effluents. This could underscore the choice of filtration media, with bark and biochar media mitigating the release of MPs even at increased flow intensities.

The effluent counts of MPs from the biochar filters first replica decreased when increasing the filter length from 25 to either 50 or 100 cm. At 25 cm, the effluent concentration was 100 MP/L which decreased to 54 and 67 MP/L for the 50 and 100 cm filters, respectively. For the second replica, this behavior was reversed with decreased effluent MP concentrations when increasing the filter length from 25 cm to either 50 or 100 cm. Effluent counts of 35 MP/L was measured for the 25 cm filter, which increased to 355 and 110 MP/L for the 50 and 100 cm filters, respectively (Fig. 4). The largest effluent MP concentrations were expected for the shortest filters, given that there was less material to capture and prohibit the MP horizontal transport. However, for biochar, the highest effluent MP count was found in one of the 50 cm filters. Despite this, there was no distinct increase in the average mass of MPs/L passing through the 50 cm filter. This suggests that the effluents in the 50 cm filter were comprised of larger-sized MPs, specifically PE and PP. Notably, 3 and 4% of PP and PE counts contributed to 53% of the effluent MP mass concentrations.

In all effluents, the highest effluent count was measured in the first replicate of the 25 cm bark filter, with 748 MP/L, which greatly decreased to 15 MP/L in the 50 cm filter and 40 MP/L in the 100 cm filter. However, the second replicate showed effluent MP counts almost 50 times less than the first 25 cm replicate, providing 15 MP/L, and

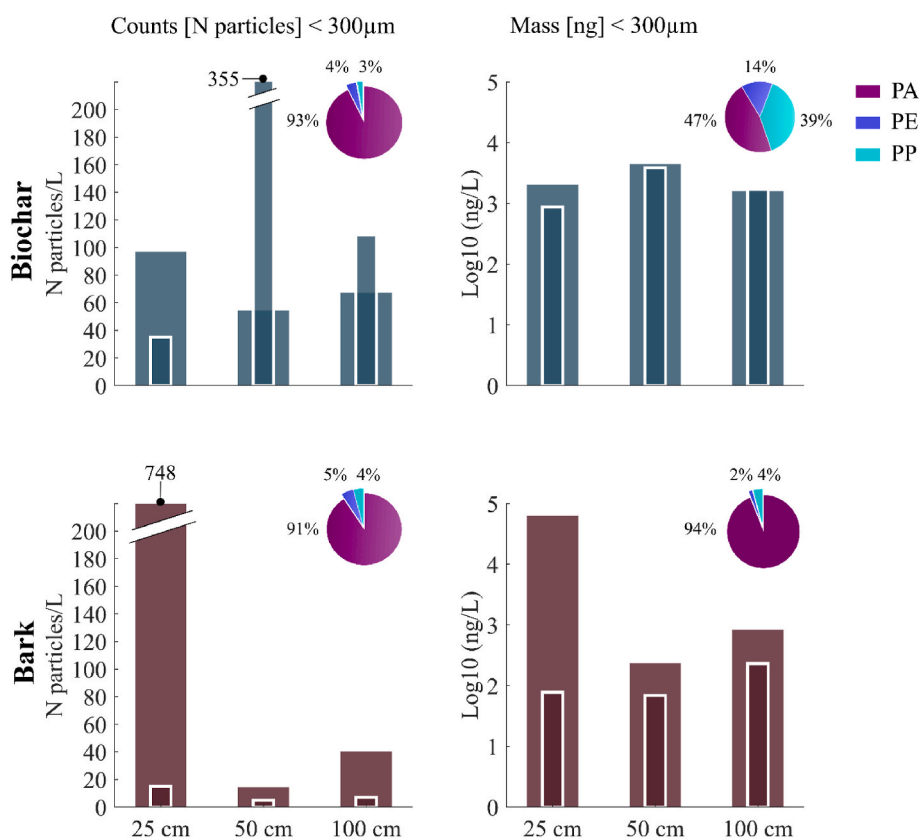


Fig. 4. Counts and mass estimations of effluent particles (PA, PE, and PP) per liter, quantified for bark and biochar of 25, 50, and 100 cm filters. Replicas 1 and 2 of each experiment are plotted transposed to each other, with thicker bars representing replica 1 and the thinner bars showing replica 2. The pie charts represent the average polymer distribution (%) of counts and mass for all filter lengths and replicas in biochar and bark filters ($n = 6$).

decreased for 50 and 100 cm filters with MP counts close to the background levels measured in the controls, thus being neglectable. In similarity with the biochar filters, the particle distribution of the average mass of effluent MPs from bark filters, revealed that most, 94%, of the MPs were PAs, with the majority of these concentrated in the effluent from the first replicate of the 25 cm filter (Fig. 4). A decrease in effluent with increased filter length was noted when we combined all data (replicas and materials) showing mean MP count concentrations decreasing from 224, 107 and 55 MP/L for 25, 50 and 100 cm filter lengths. However, it is crucial to note that this observtaion is heavily influenced by two filter replicas: one 25 cm bark filter and one 50 cm biochar filter, both exhibiting considerably larger effluent concentrations than their counterparts. This introduced a variability in effluent data. One potential explanation for this large variation between filter replicas could be an inconsistent packing of filters, resulting in air pockets and preferential pathways for MPs to transport through the filters. Although variations in 50 cm biochar filter replicas occurred, they were less than what was found for the 25 cm bark filters. This could be an added advantage of the material's polydispersity. The specific structure of pores and particle sizes of biochar depend on production methods and mother material, making it more versatile for the removal of various types and sizes of pollutants and a greater consistency in packing.

In this study, tracer tests were conducted on the control systems, revealing residence times comparable to the theoretically calculated values (see Supplementary Information S3), with the largest differences being 81 and 60 min for the 25 cm filters of bark and biochar, respectively. The difference between theoretical and measured values could be attributed to small differences in the packing of filters, or measurement uncertainties. Due to the higher porosity of biochar compared to bark, the theoretical residence time was slightly longer for biochar filters. However, given that the experiment was carried out with several pore volumes for each filter, it is unlikely that this difference had any noteworthy influence on the horizontal transport of MPs when comparing the two filter materials. Still, the variability in the MP effluents between filter replicas of bark and biochar, underscores the importance of filter packing. Therefore, it is recommended that tracer tests be conducted for each filter, prior to future experiments, preferably with repetition. Such an approach could help identify potential complications with packing, including preferential pathways.

As expected, the specific surface area of biochar was much greater, $158 \text{ m}^2/\text{g}$, than the bark's of $0.75 \text{ m}^2/\text{g}$ (Table 1). But when comparing the counts and masses of MPs in filter effluents, the results do not indicate any distinct advantage for biochar in terms of limiting effluent MPs. Nor did the difference in the measured average intragranular pore diameter of the materials, bark (17.2 nm) and biochar (3.6 nm; Table 1), seem to make a significant impact on the results. These pore sizes were considerably smaller than the smallest MP used in this study (25 μm), suggesting that they may not have had much effect on MP retention. Instead, the retention is expectedly more governed by the macro-pores and average grain sizes of the filters (DeNovio et al., 2004). However, the presence of nanopores presents an opportunity for the sorption materials to capture smaller-scaled MPs or NPs, especially with prolonged filter operations where retained MPs may weather and fragment over time (Munoz et al., 2022).

Excluding the instance of high MP effluent found in one 25 cm bark filter, the lowest MP effluents were observed for bark filters compared to biochar filters, regardless of filter length. From the elemental composition, bark showed higher levels of oxygen (33.3%) than biochar (12.9%; Table 1). This is expected, as volatile and polar surface functional groups can be driven off during the pyrolysis process of producing biochar, hence increasing C content whilst losses of O and H occur (Cantrell et al., 2012). At the same time, bark has a specific protective function in the environment and may contain naturally soluble polar polyphenolic compounds, such as tannins, which protect trees from external forces, serving as a shield for harsh environments or pests (Kemppainen et al.,

2014). Compared to the non-polar PE, PP, and PS MPs (Zhao et al., 2020) used in this study, the small-sized PA contains amide groups that are known to display polarity (Endo et al., 2011), thereby lowering its hydrophobicity (Liu et al., 2019b). Being that PA was the dominant MP by counts to transport through the biochar filters, it is suggested that the interaction between polyphenolic compounds and PA in bark filters could have impacted their transport. The effect of polyphenolic compounds on small-sized MPs retention by surface adsorption has been shown previously (Wang et al., 2023)

3.3. Microplastics retained in bark segments

By dissecting a 100 cm bark filter, a better understanding of the retention and transport of the MPs within the filter media could be derived. Given the difficulties of extracting MPs from the solid materials (see section 2.4 in the Methods), the quantification of MPs in this section will not be discussed in absolute counts or masses, or as a tool for mass balance. Instead, it should be viewed as a relative comparison of MP content between segments of the bark filter. It is still believed that the proposed extraction method can provide additional information on the horizontal distribution of MP in the bark, as the same extraction method was applied to all segments, systematically.

For the largest MPs (PS; 900 μm), 90% of all PS beads remained in the first 0–10 cm segment and 7% of the extracted PS (135 beads) had transported between the 10–100 cm bark segments, of which 5% retained in the 10–20 cm segment and 2% made their way to the 90–100 cm segment (Fig. 5). Still, no PS was found in effluents of any bark or biochar filters. Despite the uncertainty related to the extraction of MPs from the bark, 70% of the initial input of PS beads (0.5 g) could be recovered by manual collection. There are many reasons for this MP loss, with the foremost being human error associated with the manual picking

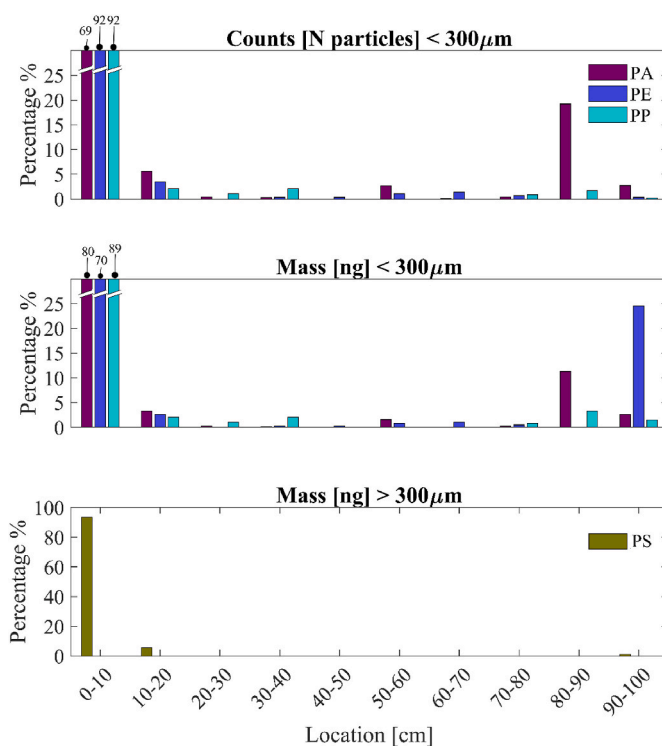


Fig. 5. The percentage distribution of retained MP types per 10 cm segments of a 100 cm bark filter. The first two figures show the percentual MP distribution of PA, PE, and PP MPs for the counts and estimated masses of polymers in each segment. Note the break in the Y-axis, introduced for increased interpretation of low percentual results. The last graph shows the actual weight distribution of PS beads which were extracted and manually picked for each segment. The sum of individual MP types from all segments is 100%.

and counting of PS. However, the recovery of PS beads was 100% in the recovery experiment, showing some reliability of the extraction method.

For particles smaller than 300 μm (PA, PE, and most PP), 69–92% of the MP counts (70–89% on a mass basis) remained in the 0–10 cm segment of the bark filter (Fig. 5). In detail, the percentual distribution of PA counts decreased from 69% in the 0–10 cm segment to 6% in the 10–20 cm segment. PA was identified in all bark segments except for 40–50 cm and showed declining distribution within the 20–80 cm segments. Thereafter, an abrupt increase in the PA prevalence (19%) was found in the 80–90 cm segment before decreasing again to 2.7% in the last section (90–100 cm) of the filter.

A similar trend was noticed for PE and PP, where most MPs were found in 0–10 cm. The most concentrated segment content, apart from 0 to 10 cm, was found for PE in the 90–100 cm segment, which comprised almost 24% of the total estimated mass of PE in the filter (Fig. 5). However, this percentual mass only corresponds to 0.34% of the total PE counts in the filter. The mean major dimension of PE in the 90–100 cm segment was 253 μm , meaning that the particles found in this segment deviated from the average particle size distribution (125 μm), provided by the vendor. Considering the analytical method applied, visual images suggest that the larger PE sizes refer to single particles, and not agglomerations of MPs, which can otherwise occur between particles of low repulsion forces and hydrophobic nature (Summers et al., 2018).

The bark contained fine particles ($D_{10} = 0.7$ mm; Fig. 1). Some of the fine bark particles were likely displaced when packing the filters in a vertical position, which could have led to compaction of the bark in the lower end. This suggests smaller pores in the 80–100 cm segment compared to the other segments. Under such conditions, the MPs that were transported through the filter length could have been trapped in the compacted zone.

3.4. Porous media filtration mechanisms and effects on microplastic removal

This experiment utilizes bark and biochar media with particles ranging from 0.5 to 4.5 mm, and should be seen as a comparison between the efficiency of filter materials, rather than a real-world filtration system. The particle size distributions in this study were guided by recommendations for colder climates, aiming for an effective particle diameter (D_{10}) larger than 0.5 mm to ensure efficient infiltration, particularly in winter months (Blecken, 2016; Moghadas et al., 2016). Considerations were made to prevent issues such as particle migration and structural collapse, especially given the fragile nature of biochar and the potential softening of bark material over time (FAWB, 2009). Therefore, media particle sizes (Fig. 1) were designed to ensure an infiltration rate, typically 50–300 mm/h (Hunt et al., 2012; Larm & Blecken, 2019), to target the removal of MPs while mitigating clogging, common in infiltration systems. This study found a high, >97%, retention of a mixture of MPs in both bark and biochar filters, influenced by various factors, including media grain size distributions and texture. Notably, the characteristics of the filter media play a crucial role in MP retention. Sandy soils, for instance, exhibit a higher distribution of aerated pores compared to finer soils, thus facilitating increased MP transport (Yu et al., 2021). Similarly, larger pore distributions in filter media can result in preferential pathways that favor MP transport (Zubris & Richards, 2005). This suggested process likely contributed to the observed variation in filtration efficiency found in the study (Fig. 4).

The filter media can also influence the pH. Here, the alkalinity of biochar contrasts the acidic nature of bark. During the experiment, pH in the effluents from biochar and bark increased from 7.7 to 8.1 and 4.7 to 7.4, respectively, falling within the pH range typically measured in stormwater (Table 1; Duncan, 1999). This increase in the pH of bark filters may be due to filter washing (Khiari et al., 2020), with leaching of organic acids and tannins from the bark filters. Notably, the bark effluent showed a decrease of yellow tint over time, shown in bark filters

elsewhere (Dalahmeh et al., 2012). The effect of MPs on pH in biochar and bark filters is still uncertain, as studies have shown that MPs can both increase and decrease pH in soil (Boots et al., 2019; Qi et al., 2020). Although this study did not include the assessment of pH in the effluents, it is important when considering the removal of other stormwater pollutants such as metals, and even smaller plastic particles such as NPs. For instance, Wang et al. (2022) related an increased pH from 5 to 9 with increased mobility of PS particles (50–500 nm) in sand column studies. This increase in mobility is explained by an enhanced electrostatic repulsion between the sand and plastic particles at the higher pH. In this study the smallest measured MPs are 25 μm , and are therefore believed to be physically retained in the biochar and bark media.

The retention behavior of MPs in porous media is influenced by their size relative to the average media grain size, with straining becoming increasingly dominant as the MP-to-grain particle size ratio decreases. Bradford et al. (2002) suggest that a particle diameter to mean grain size ratio larger than 0.002 allows for straining. In this study, the smallest MP-to-grain particle size ratio is observed with PA (25 μm), resulting in ratios larger than 0.009 and 0.011 for biochar and bark media, respectively. This suggests that the high retention of MPs observed in this experiment can be caused by straining, wherein MPs are retained in pore throats or grain junctions smaller than their average size. However, Sakthivadivel (1969) suggests that straining occurs when the particle size of MPs exceeds 5% of the average grain size. This implies that straining would be dominant for PP, PE and PS MPs larger than 110 and 130 μm in bark and biochar filters, respectively. This raises questions regarding the retention mechanisms for small-scaled PA (Fig. 6). It is plausible that MPs retained during transport could gradually block otherwise passable pores, narrowing the passageway for PA (Hou et al., 2020). In a similar notion, hydrophobic MPs can aggregate during their flow path, increasing their overall size and tendency to retain in the media, while the high concentration of MPs utilized in the experiment might cause bridging resulting in PA retention in pore throats (Khilar et al., 1983).

With excessive straining, some pores may become dead-ends, resulting in clogging, which is common near filter surfaces (Bradford et al., 2003). Such mechanical filtration likely explains the retention of large PS beads (900 μm) observed in the 0–10 cm bark media (Bradford et al., 2002). Notably, some of these large PS beads was present in the 80–90 cm bark segment, indicating the existence of preferential pathways, which likely enabled the transport of MPs, including PA, through the filters.

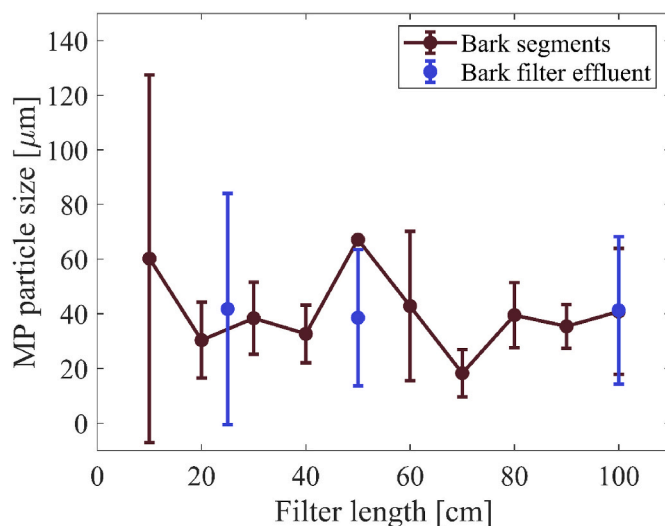


Fig. 6. Error bars represents the combined mean and standard deviation of PA, PE and PP MP particle size, measured as Feret minimum, extracted from bark segments and effluent from bark filters of 25, 50 and 100 cm.

3.5. Retention of microplastics and its implications

The largest effluent MP counts of PA, PE, and PP were observed in the first replica of 25 cm bark filters, corresponding to a removal of 97.2–98.9%, based on MP counts. Similarly, the first replica of a 100 cm bark filter retained 98.5% of PA whilst removing >99% of the remaining MP types. All other filters and replicas provided retentions of PA, PE, and PP larger than 99% for all filters, regardless of filter length and material (for details, view [Supplementary Information S6](#)). In all cases, 100% of PS beads were retained.

Biochar and bark filters provided high removals of a wide size range of MPs (25–900 μm), in accordance with available studies ([Siipola et al., 2020](#); [Wang et al., 2020](#)). The results indicate that MP mobility in the horizontal flow filters correlated to MP size, as no PS (900 μm) was found in any effluent, and the smallest MP, PA (25 μm), was the dominant MP in the effluent of all filter lengths, materials, and replicas when compared to their distribution in the initial layers of filter inlets ([Figs. 3 and 4](#)). The evidence that smaller-sized MPs have greater mobility has been previously reported in both vertical ([Rillig et al., 2017a](#); [Rillig et al., 2017b](#)) and horizontal flow experiments ([Rullander et al., 2023](#)). Despite this, there was no distinct difference between the counts of PP (63 μm) and PE (125 μm) analyzed in effluents. These observations may lead to the conclusion that the irregular shape of PP could have increased the MP's tendency to entangle in the bark and biochar filters compared to the spherical MP shape, which has been suggested in prior studies ([O'Connor et al., 2019](#); [Yao et al., 1971](#)). While the influence of particle shape on MP retention is well documented, it becomes especially evident when considering MP fibers. Due to their elongated morphology and high length to width ratio, their retention in filters is linked to their particular orientation, making it unclear how their mobility compares to other MP shapes ([Cohen & Radian, 2022](#)).

A similar horizontal flow study of sand material, operating at lower flow, observed an equally high removal of MPs as provided by the bark and biochar filters ([Rullander et al., 2023](#)). Although high porosity organic filters exhibited a similar MP removal relative to sand filters, sand media have also been shown to be inferior in removing and binding smaller particles and colloids in stormwater, especially when stormwater contaminants with contrasting properties ([Grebel et al., 2013](#); [Kalmykova et al., 2014](#)). Additionally, the benefits of incorporating organic materials include the positive aspects of carbon sequestration and utilization of forestry waste products. Similarly, the longevity and circular reusability of the carbon byproducts can be further impactful when considering the possibilities of multiple uses. That is, pyrolyzing bark material from exhausted filters and re-applying the produced biochar once again as a filter media ([Sessa et al., 2022](#)), with options to recover sorbed metals from combusted ashes via chemical washing ([Fedje et al., 2015](#)).

Since no linear relationship has been established between MP concentration in initial layers and MP transport ([O'Connor et al., 2019](#)), this paper mostly focused on the difference in effluent counts per liter effluents, instead of percentual removal. This approach highlights the potential impact of effluent MPs, indicating that even a small percentage of MPs in treated effluents can contribute to environmental pollution. This is important, as stormwater can be a significant source of MPs.

3.6. Limitations of the study

This experiment was conducted in a laboratory setting and has limitations in replicating real-world scenarios, particularly in urban environments where stormwater quality and flow rates vary. While the study examines virgin MPs, it is important to recognize that real-world MPs often undergo natural weathering, which can impact their behavior and retention in stormwater filtration systems. Moreover, this study analyzed segments of a 100 cm bark filter, but was limited to one filter. It is suggested that further studies with larger sample sizes could help to expand the knowledge gathered in this study.

As discussed previously, the size of MPs greatly affects their tendency to be retained in filter media. Although μFTIR imaging can be used to analyze MP particles as small as 25 μm , its accuracy is limited to MPs larger than 10 μm . This highlights the necessity for retention studies on smaller-sized MPs using high porosity materials, especially since MP concentration tend to increase with decreased particle size in stormwater. Additionally, subsampling and extrapolation of data obtained from μFTIR imaging may affect accuracy, while estimating MP mass using SiMPLE may overestimate the volumes of certain MPs due to the assumption of elliptical MP volumes. Complementing this analysis with techniques such as pyrolysis GC-MS could provide more accurate data on MP mass, particularly for fragmented PP particles. Using such analytical techniques could also facilitate the examination of tire wear particles, which are known to be abundant in stormwater, particularly in road runoff ([Järllskog et al., 2022](#)).

4. Conclusion

The results of this study, including the dissection of a 100 cm bark filter, indicate that MPs (25–900 μm) are greatly retained in the horizontal-flow filters, especially in the first layer of the analyzed bark filter (0–10 cm). Bark and biochar filters showed overall high retention of PA, PE, and PP (>97%), with a 100% removal of large-sized (900 μm) PS beads. Still, PA, PE, and PP MPs were detected in all effluents, with varying effluent MP counts of 5–750 MP/L and 35–355 MP/L for bark and biochar filters of lengths 25, 50, and 100 cm. The highest effluent MP counts measured in the study were derived from a 25 and 50 cm filter of bark and biochar, respectively. Thus, implying that longer filters of 100 cm can serve a purpose in minimizing MP pollution, while consistent packing of filters to minimize accidental channeling in the porous materials is stressed. It is important to note that a minor percentage release of MPs from filtration units can still be a large contributor to MP emissions, particularly in cases of highly polluted stormwater. The conclusion remains that the benefits of utilizing bark and biochar material are promising and that sustainably sourced organic materials should be considered for MP removal as stormwater filters.

Funding sources

The work presented in this article is part of the activities implemented within the project “Cities with less microplastics: Road-side green filters to remove microplastics from urban stormwater”, which was funded by the Swedish Research Council for Environment, Agricultural Sciences and Spatial Planning (FORMAS), grant number 2019-01911.

CRedit authorship contribution statement

Gabriella Rullander: Writing – review & editing, Writing – original draft, Visualization, Project administration, Methodology, Investigation, Formal analysis, Data curation, Conceptualization. **Claudia Lorenz:** Writing – review & editing, Validation, Supervision, Project administration, Methodology, Conceptualization. **Ann-Margret Strömvall:** Writing – review & editing, Validation, Supervision, Project administration, Methodology, Investigation, Conceptualization. **Jes Vollertsen:** Writing – review & editing, Supervision, Project administration, Methodology, Conceptualization. **Sahar S. Dalahmeh:** Writing – review & editing, Supervision, Resources, Project administration, Methodology, Funding acquisition.

Declaration of competing interest

The authors declare that they have no known competing financial interests or personal relationships that could have appeared to influence the work reported in this paper.

Data availability

Data will be made available on request.

Acknowledgments

We extend our gratitude to Associate Professor Roger Herbert at the department of Earth Sciences (Uppsala university) in proofreading of the manuscript. Additionally, we show gratitude towards Lagerträder (Uppsala university), for their help in building the experimental set-ups.

Appendix A. Supplementary data

Supplementary data to this article can be found online at <https://doi.org/10.1016/j.envpol.2024.124335>.

References

- Amenábar, M., Aguilera, M.A., Gallardo, C., Moore, C., De Vine, R., Lattin, G., Gamba, A., Luna-Acosta, A., Thiel, M., 2024. Spatial distribution of microplastics in a coastal upwelling region: offshore dispersal from urban sources in the Humboldt Current System. *Environ. Pollut.* 343, 123157 <https://doi.org/10.1016/j.envpol.2023.123157>.
- Arole, K., Velhal, M., Tajedini, M., Xavier, P.G., Bardasz, E., Green, M.J., Liang, H., 2023. Impacts of particles released from vehicles on environment and health. *Tribol. Int.* 184, 108417 <https://doi.org/10.1016/j.triboint.2023.108417>.
- Ashoori, N., Teixeira, M., Spahr, S., LeFevre, G.H., Sedlak, D.L., Luthy, R.G., 2019. Evaluation of pilot-scale biochar-amended woodchip bioreactors to remove nitrate, metals, and trace organic contaminants from urban stormwater runoff. *Water Res.* 154, 1–11. <https://doi.org/10.1016/j.watres.2019.01.040>.
- Bansal, R.C., Goyal, M., 2005. *Activated Carbon Adsorption*. CRC press.
- Bibi, T.S., Kara, K.G., 2023. Evaluation of climate change, urbanization, and low-impact development practices on urban flooding. *Heliyon* 9 (1), e12955. <https://doi.org/10.1016/j.heliyon.2023.e12955>.
- Biswal, B.K., Vijayaraghavan, K., Tsen-Tieng, D.L., Balasubramanian, R., 2022. Biochar-based bioretention systems for removal of chemical and microbial pollutants from stormwater: a critical review. *J. Hazard Mater.* 422, 126886 <https://doi.org/10.1016/j.jhazmat.2021.126886>.
- Björklund, K., Li, L., 2015. Evaluation of low-cost materials for sorption of hydrophobic organic pollutants in stormwater. *J. Environ. Manag.* 159, 106–114. <https://doi.org/10.1016/j.jenvman.2015.05.005>.
- Blecken, G., 2016. *Kunskapsmanställning Dagvattenrening*, p. 104, 2016–05. www.svenskvatten.se.
- Boots, B., Russell, C.W., Green, D.S., 2019. Effects of microplastics in soil ecosystems: Above and below ground. *Environmental Science & Technology* 53 (19), 11496–11506.
- Bradford, S.A., Simunek, J., Bettahar, M., van Genuchten, M. Th, Yates, S.R., 2003. Modeling colloid attachment, straining, and exclusion in saturated porous media. *Environ. Sci. Technol.* 37 (10), 2242–2250. <https://doi.org/10.1021/es025899u>.
- Bradford, S.A., Yates, S.R., Bettahar, M., Simunek, J., 2002. Physical factors affecting the transport and fate of colloids in saturated porous media. *Water Resour. Res.* 38 (12), 63, 1.
- Brás, I., Teixeira Lemos, L., Alves, A., Fernando, R., Pereira, M., 2004. Application of pine bark as a sorbent for organic pollutants in effluents. *Manag. Environ. Qual. Int. J.* 15 (5), 491–501.
- Cantrell, K.B., Hunt, W.F., Uchimiya, M., Novak, J.M., Ro, K.S., 2012. Impact of pyrolysis temperature and manure source on physicochemical characteristics of biochar. *Bioresour. Technol.* 107, 419–428.
- Chandrasena, G.I., Shirdashtzadeh, M., Li, Y.L., Deletic, A., Hathaway, J.M., McCarthy, D.T., 2017. Retention and survival of *E. coli* in stormwater biofilters: role of vegetation, rhizosphere microorganisms and antimicrobial filter media. *Ecol. Eng.* 102, 166–177. <https://doi.org/10.1016/j.ecoleng.2017.02.009>.
- Cohen, N., Radian, A., 2022. Microplastic textile fibers accumulate in sand and are potential sources of micro(nano)plastic pollution. *Environ. Sci. Technol.* 56 (24), 17635–17642. <https://doi.org/10.1021/acs.est.2c05026>.
- Coyle, R., Hardiman, G., Driscoll, K.O., 2020. Microplastics in the marine environment: a review of their sources, distribution processes, uptake and exchange in ecosystems. *Case Studies in Chemical and Environmental Engineering* 2, 100010. <https://doi.org/10.1016/j.csee.2020.100010>.
- Dalahmeh, S.S., Pell, M., Vinnerås, B., Hylander, L.D., Öborn, I., Jönsson, H., 2012. Efficiency of bark, activated charcoal, foam and sand filters in reducing pollutants from greywater. *Water, Air, Soil Pollut.* 223 (7), 3657–3671. <https://doi.org/10.1007/s11270-012-1139-z>.
- Davis, A.P., Hunt, W.F., Traver, R.G., Clar, M., 2009. Bioretention technology: overview of current practice and future needs. *J. Environ. Eng.* 135 (3), 109–117. [https://doi.org/10.1061/\(ASCE\)0733-9372\(2009\)135:3\(109\)](https://doi.org/10.1061/(ASCE)0733-9372(2009)135:3(109)).
- DeNovio, N.M., Saiers, J.E., Ryan, J.N., 2004. Colloid movement in unsaturated porous media: recent advances and future directions. *Vadose Zone J.* 3 (2), 338–351. <https://doi.org/10.2136/vzj2004.0338>.
- Dobaradaran, S., Schmidt, T.C., Lorenzo-Parodi, N., Kaziru-Cegla, W., Jochmann, M.A., Nabipour, I., Lutze, H.V., Telgheder, U., 2020. Polycyclic aromatic hydrocarbons (PAHs) leachates from cigarette butts into water. *Environ. Pollut.* 259, 113916 <https://doi.org/10.1016/j.envpol.2020.113916>.
- Duncan, H., 1999. *Urban Stormwater Quality: A Statistical Overview*. CRC for Catchment Hydrology.
- Enders, K., Lenz, R., Stedmon, C.A., Nielsen, T.G., 2015. Abundance, size and polymer composition of marine microplastics $\geq 10 \mu\text{m}$ in the Atlantic Ocean and their modelled vertical distribution. *Mar. Pollut. Bull.* 100 (1), 70–81. <https://doi.org/10.1016/j.marpolbul.2015.09.027>.
- Endo, S., Droge, S.T., Goss, K.-U., 2011. Polyparameter linear free energy models for polyacrylate fiber– water partition coefficients to evaluate the efficiency of solid-phase microextraction. *Anal. Chem.* 83 (4), 1394–1400.
- Epa, S., 1999. *Storm Water Technology Fact Sheet-Bioretenion*. Office of Water, p. 12. EPA 832-F-99.
- Fedje, K.K., Modin, O., Strömvall, A.-M., 2015. Copper recovery from polluted soils using acidic washing and bioelectrochemical systems. *Metals* 5 (3), 1328–1348. <https://doi.org/10.3390/met5031328>.
- Goor, J., Cantelon, J., Smart, C.C., Robinson, C.E., 2021. Seasonal performance of field bioretention systems in retaining phosphorus in a cold climate: influence of prolonged road salt application. *Sci. Total Environ.* 778, 146069 <https://doi.org/10.1016/j.scitotenv.2021.146069>.
- Grebel, J., Mohanty, S., Torkelson, A., Boehm, A., Higgins, C., Maxwell, R., Nelson, K., Sedlak, D., 2013. Engineered infiltration systems for urban stormwater reclamation. *Environ. Eng. Sci.* 30, 437–454. <https://doi.org/10.1089/ees.2012.0312>.
- Hou, J., Xu, X., Lan, L., Miao, L., Xu, Y., You, G., Liu, Z., 2020. Transport behavior of micro polyethylene particles in saturated quartz sand: impacts of input concentration and physicochemical factors. *Environ. Pollut.* 263, 114499 <https://doi.org/10.1016/j.envpol.2020.114499>.
- Hunt, W.F., Davis, A.P., Traver, R.G., 2012. Meeting hydrologic and water quality goals through targeted bioretention design. *J. Environ. Eng.* 138 (6), 698–707.
- Iannuzzi, Z., Mourier, B., Winiarski, T., Lipeme-Kouyi, G., Polomé, P., Bayard, R., 2024. Contribution of different land use catchments on the microplastic pollution in detention basin sediments. *Environ. Pollut.* 348, 123882 <https://doi.org/10.1016/j.envpol.2024.123882>.
- Järllskog, I., Jaramillo-Vogel, D., Rausch, J., Gustafsson, M., Strömvall, A.-M., Andersson-Sköld, Y., 2022. Concentrations of tire wear microplastics and other traffic-derived non-exhaust particles in the road environment. *Environ. Int.* 170, 107618 <https://doi.org/10.1016/j.envint.2022.107618>.
- Järllskog, I., Strömvall, A.-M., Magnusson, K., Gustafsson, M., Polukarova, M., Galfi, H., Aronsson, M., Andersson-Sköld, Y., 2020. Occurrence of tire and bitumen wear microplastics on urban streets and in sweepsand and washwater. *Sci. Total Environ.* 729, 138950 <https://doi.org/10.1016/j.scitotenv.2020.138950>.
- Johansson, G., Fedje, K.K., Modin, O., Haeger-Eugensson, M., Uhl, W., Andersson-Sköld, Y., Strömvall, A.-M., 2024. Removal and release of microplastics and other environmental pollutants during the start-up of bioretention filters treating stormwater. *J. Hazard Mater.*, 133532 <https://doi.org/10.1016/j.jhazmat.2024.133532>.
- Kalmykova, Y., Moona, N., Strömvall, A.-M., Björklund, K., 2014. Sorption and degradation of petroleum hydrocarbons, polycyclic aromatic hydrocarbons, alkylphenols, bisphenol A and phthalates in landfill leachate using sand, activated carbon and peat filters. *Water Res.* 56, 246–257.
- Kemppainen, K., Siika-aho, M., Pattathil, S., Giovando, S., Kruus, K., 2014. Spruce bark as an industrial source of condensed tannins and non-cellulosic sugars. *Ind. Crop. Prod.* 52, 158–168. <https://doi.org/10.1016/j.indcrop.2013.10.009>.
- Khiari, Z., Alka, K., Kelloway, S., Mason, B., Savidou, N., 2020. Integration of biochar filtration into aquaponics: effects on particle size distribution and turbidity removal. *Agric. Water Manag.* 229, 105874 <https://doi.org/10.1016/j.agwat.2019.105874>.
- Khilar, K.C., Fogler, H.S., Ahluwalia, J.S., 1983. Sandstone water sensitivity: existence of a critical rate of salinity decrease for particle capture. *Chem. Eng. Sci.* 38 (5), 789–800. [https://doi.org/10.1016/0009-2509\(83\)80188-2](https://doi.org/10.1016/0009-2509(83)80188-2).
- Krahn, K.M., Cornelissen, G., Castro, G., Arp, H.P.H., Asimakopoulos, A.G., Wolf, R., Holmstad, R., Zimmerman, A.R., Sormo, E., 2023. Sewage sludge biochars as effective PFAS-sorbents. *J. Hazard Mater.* 445, 130449 <https://doi.org/10.1016/j.jhazmat.2022.130449>.
- Kuoppamäki, K., Pflugmacher Lima, S., Scopetani, C., Setälä, H., 2021. The ability of selected filter materials in removing nutrients, metals, and microplastics from stormwater in biofilter structures. *J. Environ. Qual.* 50 (2), 465–475. <https://doi.org/10.1002/jeq2.20201>.
- Lange, K., Magnusson, K., Viklander, M., Blecken, G.-T., 2021. Removal of rubber, bitumen and other microplastic particles from stormwater by a gross pollutant trap—bioretention treatment train. *Water Res.* 202, 117457 <https://doi.org/10.1016/j.watres.2021.117457>.
- Larm, T., Blecken, G., 2019. *Utförning Och Dimensionering Av Anläggningar För Rening Och Flödesutjämning Av Dagvatten*, p. 116, 2019–20. www.svenskvatten.se.
- Li, H., Dong, X., da Silva, E.B., de Oliveira, L.M., Chen, Y., Ma, L.Q., 2017. Mechanisms of metal sorption by biochars: biochar characteristics and modifications. *Chemosphere* 178, 466–478. <https://doi.org/10.1016/j.chemosphere.2017.03.072>.
- Li, Y., Chen, B., Zhu, L., 2010. Enhanced sorption of polycyclic aromatic hydrocarbons from aqueous solution by modified pine bark. *Bioresour. Technol.* 101 (19), 7307–7313. <https://doi.org/10.1016/j.biortech.2010.04.088>.
- Liu, F., Vianello, A., Vollertsen, J., 2019. Retention of microplastics in sediments of urban and highway stormwater retention ponds. *Environ. Pollut.* 255, 113335 <https://doi.org/10.1016/j.envpol.2019.113335>.
- Liu, X., Xu, J., Zhao, Y., Shi, H., Huang, C.-H., 2019. Hydrophobic sorption behaviors of 17 β -Estradiol on environmental microplastics. *Chemosphere* 226, 726–735. <https://doi.org/10.1016/j.chemosphere.2019.03.162>.

- Markiewicz, A., Strömwall, A.-M., Björklund, K., 2020. Alternative sorption filter materials effectively remove non-particulate organic pollutants from stormwater. *Sci. Total Environ.* 730, 139059 <https://doi.org/10.1016/j.scitotenv.2020.139059>.
- Masura, J., Baker, J.E., Foster, G.D., Gregory, D., Arthur, C., Herring, C., 2015. Laboratory methods for the analysis of microplastics in the marine environment: recommendations for quantifying synthetic particles in waters and sediments. <https://repository.library.noaa.gov/view/noaa/10296>.
- Milovanovic, I., Herrmann, I., Hedström, A., Nordqvist, K., Müller, A., Viklander, M., 2023. Synthetic stormwater for laboratory testing of filter materials. *Environ. Technol.* 44 (11), 1600–1612. <https://doi.org/10.1080/09593330.2021.2008516>.
- Moghadas, S., Gustafsson, A.-M., Viklander, P., Marsalek, J., Viklander, M., 2016. Laboratory study of infiltration into two frozen engineered (sandy) soils recommended for bioretention. *Hydrol. Process.* 30 (8), 1251–1264. <https://doi.org/10.1002/hyp.10711>.
- Mohanty, S.K., Valenca, R., Berger, A.W., Yu, I.K.M., Xiong, X., Saunders, T.M., Tsang, D. C.W., 2018. Plenty of room for carbon on the ground: potential applications of biochar for stormwater treatment. *Sci. Total Environ.* 625, 1644–1658. <https://doi.org/10.1016/j.scitotenv.2018.01.037>.
- Monira, S., Roychand, R., Bhuiyan, M.A., Hai, F.I., Pramanik, B.K., 2022. Identification, classification and quantification of microplastics in road dust and stormwater. *Chemosphere* 299, 134389. <https://doi.org/10.1016/j.chemosphere.2022.134389>.
- Munoz, L.P., Baez, A.G., Purchase, D., Jones, H., Garelick, H., 2022. Release of microplastic fibres and fragmentation to billions of nanoplastics from period products: preliminary assessment of potential health implications. *Environ. Sci.: Nano* 9 (2), 606–620.
- O'Brien, S., Okoffo, E.D., Rauert, C., O'Brien, J.W., Ribeiro, F., Burrows, S.D., Toapanta, T., Wang, X., Thomas, K.V., 2021. Quantification of selected microplastics in Australian urban road dust. *J. Hazard Mater.* 416, 125811 <https://doi.org/10.1016/j.jhazmat.2021.125811>.
- O'Connor, D., Pan, S., Shen, Z., Song, Y., Jin, Y., Wu, W.-M., Hou, D., 2019. Microplastics undergo accelerated vertical migration in sand soil due to small size and wet-dry cycles. *Environ. Pollut.* 249, 527–534. <https://doi.org/10.1016/j.envpol.2019.03.092>.
- Olesen, K.B., Stephansen, D.A., van Alst, N., Vollertsen, J., 2019. Microplastics in a stormwater pond. *Water* 11 (7). <https://doi.org/10.3390/w11071466>.
- Park, S., Kim, J., Jeon, W.-H., Moon, H.S., 2023. Exploring the vertical transport of microplastics in subsurface environments: lab-scale experiments and field evidence. *J. Contam. Hydrol.* 257, 104215 <https://doi.org/10.1016/j.jconhyd.2023.104215>.
- Payne, E., Hatt, B., Deletic, A., Dobbie, M., McCarthy, D., Chandrasena, G., 2015. Adoption guidelines for stormwater biofiltration systems. In: Cooperative Research Centre for Water Sensitive Cities. www.watersensitivecities.org.au.
- Primpke, S., Cross, R.K., Mintenig, S.M., Simon, M., Vianello, A., Gerdts, G., Vollertsen, J., 2020. Toward the systematic identification of microplastics in the environment: evaluation of a new independent software tool (SiMPLe) for spectroscopic analysis. *Appl. Spectrosc.* 74 (9), 1127–1138. <https://doi.org/10.1177/0003702820917760>.
- Qi, Y., Ossowicki, A., Yang, X., Lwanga, E.H., Dini-Andreote, F., Geissen, V., Garbeva, P., 2020. Effects of plastic mulch film residues on wheat rhizosphere and soil properties. *Journal of Hazardous Materials* 387, 121711.
- Reddy, K.R., Xie, T., Dastgheibi, S., 2014. Adsorption of mixtures of nutrients and heavy metals in simulated urban stormwater by different filter materials. *Journal of Environmental Science and Health, Part A* 49 (5), 524–539. <https://doi.org/10.1080/10934529.2014.859030>.
- Rillig, M.C., Ingrassia, R., de Souza Machado, A.A., 2017a. Microplastic incorporation into soil in agroecosystems. *Front. Plant Sci.* 8, 1805.
- Rillig, M., Ziersch, L., Hempel, S., 2017b. Microplastic transport in soil by earthworms. *Sci. Rep.* 7 (1), 1362.
- Ross, M.S., Loutan, A., Groeneveld, T., Molenaar, D., Kroetch, K., Bujacek, T., Kolter, S., Moon, S., Huynh, A., Khayam, R., Franczak, B.C., Camm, E., Arnold, V.I., Ruecker, N. J., 2023. Estimated discharge of microplastics via urban stormwater during individual rain events. *Front. Environ. Sci.* 11. <https://www.frontiersin.org/articles/10.3389/fenvs.2023.1090267>.
- Rullander, G., Lorenz, C., Herbert, R.B., Strömwall, A.-M., Vollertsen, J., Dalahmeh, S.S., 2023. How effective is the retention of microplastics in horizontal flow sand filters treating stormwater? *J. Environ. Manag.* 344, 118690 <https://doi.org/10.1016/j.jenvman.2023.118690>.
- Sakthivadivel, R., 1969. Clogging of a granular porous medium by sediment. In: *Hydraulic Engineering Laboratory, College of Engineering, University of California*. <http://catalog.hathitrust.org/Record/100801498>.
- Sang, W., Chen, Z., Mei, L., Hao, S., Zhan, C., Zhang, W. bin, Li, M., Liu, J., 2021. The abundance and characteristics of microplastics in rainwater pipelines in Wuhan, China. *Sci. Total Environ.* 755, 142606 <https://doi.org/10.1016/j.scitotenv.2020.142606>.
- Sessa, F., Merlin, G., Canu, P., 2022. Pine bark valorization by activated carbons production to be used as VOCs adsorbents. *Fuel* 318, 123346. <https://doi.org/10.1016/j.fuel.2022.123346>.
- Siipola, V., Pflugmacher, S., Romar, H., Wendling, L., Koukkari, P., 2020. Low-cost biochar adsorbents for water purification including microplastics removal. *Appl. Sci.* 10 (3) <https://doi.org/10.3390/app10030788>.
- Simon, M., van Alst, N., Vollertsen, J., 2018. Quantification of microplastic mass and removal rates at wastewater treatment plants applying Focal Plane Array (FPA)-based Fourier Transform Infrared (FT-IR) imaging. *Water Res.* 142, 1–9. <https://doi.org/10.1016/j.watres.2018.05.019>.
- SiMPLe, 2022. *About. Simple-Plastics.Eu*. <https://simple-plastics.eu/about.html>.
- Spokas, K.A., 2010. Review of the stability of biochar in soils: predictability of O:C molar ratios. *Carbon Manag.* 1 (2), 289–303.
- Summers, S., Henry, T., Gutierrez, T., 2018. Agglomeration of nano- and microplastic particles in seawater by autochthonous and de novo-produced sources of exopolymeric substances. *Mar. Pollut. Bull.* 130, 258–267. <https://doi.org/10.1016/j.marpolbul.2018.03.039>.
- Sun, X., Jia, Q., Ye, J., Zhu, Y., Song, Z., Guo, Y., Chen, H., 2023. Real-time variabilities in microplastic abundance and characteristics of urban surface runoff and sewer overflow in wet weather as impacted by land use and storm factors. *Sci. Total Environ.* 859, 160148 <https://doi.org/10.1016/j.scitotenv.2022.160148>.
- Ulrich, B.A., Im, E.A., Werner, D., Higgins, C.P., 2015. Biochar and activated carbon for enhanced trace organic contaminant retention in stormwater infiltration systems. *Environ. Sci. Technol.* 49 (10), 6222–6230. <https://doi.org/10.1021/acs.est.5b00376>.
- Valentín, L., Kluczek-Turpeinen, B., Willför, S., Hemming, J., Hatakka, A., Steffen, K., Tuomela, M., 2010. Scots pine (*Pinus sylvestris*) bark composition and degradation by fungi: potential substrate for bioremediation. *Bioresour. Technol.* 101 (7), 2203–2209. <https://doi.org/10.1016/j.biortech.2009.11.052>.
- Vianello, A., Jensen, R.L., Liu, L., Vollertsen, J., 2019. Simulating human exposure to indoor airborne microplastics using a Breathing Thermal Manikin. *Sci. Rep.* 9 (1), 8670. <https://doi.org/10.1038/s41598-019-45054-w>.
- Wagner, S., Hüffer, T., Klöckner, P., Wehrhahn, M., Hofmann, T., Reemtsma, T., 2018. Tire wear particles in the aquatic environment—a review on generation, analysis, occurrence, fate and effects. *Water Res.* 139, 83–100. <https://doi.org/10.1016/j.watres.2018.03.051>.
- Wang, J., Sun, C., Huang, Q.-X., Chi, Y., Yan, J.-H., 2021. Adsorption and thermal degradation of microplastics from aqueous solutions by Mg/Zn modified magnetic biochars. *J. Hazard Mater.* 419, 126486 <https://doi.org/10.1016/j.jhazmat.2021.126486>.
- Wang, Y., Wang, M., Wang, Q., Wang, T., Zhou, Z., Mehling, M., Guo, T., Zou, H., Xiao, X., He, Y., Wang, X., Rojas, O.J., Guo, J., 2023. Flowthrough capture of microplastics through polyphenol-mediated interfacial interactions on wood sawdust. *Adv. Mater.* 35 (36), 2301531 <https://doi.org/10.1002/adma.202301531>.
- Wang, Y., Xu, L., Chen, H., Zhang, M., 2022. Retention and transport behavior of microplastic particles in water-saturated porous media. *Sci. Total Environ.* 808, 152154 <https://doi.org/10.1016/j.scitotenv.2021.152154>.
- Wang, Z., Sedighi, M., Lea-Langton, A., 2020. Filtration of microplastic spheres by biochar: removal efficiency and immobilisation mechanisms. *Water Res.* 184, 116165 <https://doi.org/10.1016/j.watres.2020.116165>.
- Weber, K., Quicker, P., 2018. Properties of biochar. *Fuel* 217, 240–261. <https://doi.org/10.1016/j.fuel.2017.12.054>.
- Yao, K.-M., Habibi, M.T., O'Melia, C.R., 1971. Water and waste water filtration. *Concepts and applications. Environ. Sci. Technol.* 5 (11), 1105–1112.
- Yu, L., Zhang, J., Liu, Y., Chen, L., Tao, S., Liu, W., 2021. Distribution characteristics of microplastics in agricultural soils from the largest vegetable production base in China. *Sci. Total Environ.* 756, 143860 <https://doi.org/10.1016/j.scitotenv.2020.143860>.
- Zhang, X., Chen, Y., Li, X., Zhang, Y., Gao, W., Jiang, J., Mo, A., He, D., 2022. Size/shape-dependent migration of microplastics in agricultural soil under simulated and natural rainfall. *Sci. Total Environ.* 815, 152507 <https://doi.org/10.1016/j.scitotenv.2021.152507>.
- Zhang, Y., Frimpong, A.J., Tang, J., Olayode, I.O., Kyei, S.K., Owusu-Ansah, P., Agyeman, P.K., Fayzullayevich, J.V., Tan, G., 2024. An explicit review and proposal of an integrated framework system to mitigate the baffling complexities induced by road dust-associated contaminants. *Environ. Pollut.* 349, 123957 <https://doi.org/10.1016/j.envpol.2024.123957>.
- Zhao, L., Rong, L., Xu, J., Lian, J., Wang, L., Sun, H., 2020. Sorption of five organic compounds by polar and nonpolar microplastics. *Chemosphere* 257, 127206. <https://doi.org/10.1016/j.chemosphere.2020.127206>.
- Zubris, K.A.V., Richards, B.K., 2005. Synthetic fibers as an indicator of land application of sludge. *Environ. Pollut.* 138 (2), 201–211. <https://doi.org/10.1016/j.envpol.2005.04.013>.
- FAWB, 2009. *Stormwater biofiltration systems. Adoption Guidelines. Planning, Design and Practical Implementation*, 1st. Monash University 2009. <https://watersensitivecities.org.au/wp-content/uploads/2022/04/fawb-adoption-guidelines-full-document.pdf>.